Heat Mass Transfer (2005) 41: 632–641
DOI 10.1007/s00231-004-0575-8

ORIGINAL

A. J. Chamkha · H. S. Takhar · G. Nath

Unsteady compressible boundary layer flow over a circular cone near a plane of symmetry

Received: 11 March 2004 / Accepted: 19 November 2004 / Published online: 2 March 2005
© Springer-Verlag 2005

Abstract An analysis has been performed to study the unsteady laminar compressible boundary layer governing the hypersonic flow over a circular cone at an angle of attack near a plane of symmetry with either inflow or outflow in the presence of suction. The flow is assumed to be steady at time $t=0$ and at $t>0$ it becomes unsteady due to the time-dependent free stream velocity which varies arbitrarily with time. The nonlinear coupled parabolic partial differential equations under boundary layer approximations have been solved by using an implicit finite-difference method. It is found that suction plays an important role in stabilising the fluid motion and in obtaining unique solution of the problem. The effect of the cross flow parameter is found to be more pronounced on the cross flow surface shear stress than on the streamwise surface shear stress and surface heat transfer. Beyond a certain value of the cross flow parameter overshoot in the cross flow velocity occurs and the magnitude of this overshoot increases with the cross flow parameter. The time variation of the streamwise surface shear stress is more significant than that of the cross flow surface shear stress and surface heat transfer. The suction and the total enthalpy at the wall exert strong influence on the streamwise and cross flow surface shear stresses and the surface heat transfer except that the effect of suction on the cross flow surface shear stress is small.

A. J. Chamkha
Manufacturing Engineering Department,
The Public Authority for Applied Education & Training,
Shuweikh, 70654, Kuwait

H. S. Takhar (✉)
Department of Engineering,
Manchester Metropolitan University,
Manchester, M1 5GD, U.K
E-mail: h.s.takhar@mmu.ac.uk

G. Nath
Department of Mathematics,
Indian Institute of Science,
Bangalore, 560012, India

Nomenclature

a	Velocity of sound, ms^{-1}
A	Dimensionless suction parameter $=-(3/2)^{1/2}[(\rho\ w)_w/\rho_e u_0]\ Re_x^{1/2}$
C_p	Constant pressure specific heat, J kg^{-1} K
C_v	Constant volume specific heat, J kg^{-1} K
Ec	Viscous dissipation parameter $=u^2{}_0/2H_e$
f'	Dimensionless velocity component along streamwise direction $=u/u_e$
g	Dimensionless total enthalpy $=H/H_e$
h	Specific enthalpy, J kg^{-1}
H	Total enthalpy, J kg^{-1}
k	Fluid thermal conductivity, W m^{-1} K
L	Denotes dimensionless dependent variable f' or s' or g
M_e	Mach number at the edge of the boundary layer $=V/a$
N	Product of the density–viscosity ratio $=\rho\mu/\rho_e\mu_e$
p	Static pressure, Pa
p_0	Static pressure when $\theta=0$, Pa
p_2	Denotes the curvature of the pressure distribution along the plane of symmetry, Pa
Pr	Prandtl number $=\mu_e C_p/k$
r	Cylindrical radius of the cone, m
R	Dimensionless function of dimensionless time $=1+\varepsilon\tau^2$
Re_x	Reynolds number $=u_0x/\ v_e$
s'	Dimensionless cross flow velocity profile $=v/v_e$
t	Time, s
T	Temperature, K
u,v,w	Velocity components along x, θ and z directions, respectively, ms^{-1}
u_0,v_0	Value of u and v at time $t=0$, ms^{-1}
V	Fluid velocity in the inviscid flow, ms^{-1}
x	Distance along a generator of the cone from apex, m
z	Distance normal to the surface, m

Greek symbols

α	Dimensionless cross flow parameter $= 2\xi v_0/(\rho_e \mu_e u_0^2 r^3)$
α_0	Angle of attack
β	Dimensionless parameter associated with the three-dimensional nature of the flow $= (2\xi/v_0 x) \times d(v_0 x)/d\xi$
γ	Specific heat ratio $= c_{p/c_v}$ (1.4 for air)
$\Delta\eta, \Delta\tau$	Step sizes in η and τ directions, respectively
η	Transformed coordinate normal to the surface $= (3/2)(\rho_e u_0/\mu_e x)^{1/2} \int_0^z (\rho/\rho_e) dz$
θ	Circumferential angle measured from plane of symmetry
θ_c	Semi-vertical angle of the cone
μ	Viscosity coefficient, kg m^{-1} s^{-1}
ν	Kinematic viscosity, m^2 s^{-1}
ξ	Transformed streamwise coordinate $= 3^{-1} \rho_e \mu_e u_0 (\sin \theta_c)^2 x^3$
ρ	Mass density, kg m^{-3}
τ	Dimensionless time $= (3/2)(u_0/x)t$
ω	Index in the power-law variation of viscosity coefficient

Subscripts

e	Conditions at the edge of the boundary layer
i	Initial conditions
w	Wall conditions
$'$	Prime denotes derivative with respect to η

1 Introduction

The unsteady compressible three-dimensional laminar boundary layers is encountered in many practical situations such as re-entry space shuttle, accelerated and decelerated rockets and missiles, wing of supersonic aircraft, nozzle flow etc. Unsteady viscous effects have proved to play a vital role in the stability of missiles and re-entry vehicles. Small fluctuations of the angle of attack, gas injection through the skin and ablation are boundary layer phenomena that may have catastrophic effects on the stability of the body. In order to determine the frictional drag and the rate of heat transfer through the surface, the unsteady compressible three-dimensional boundary layer equations with four independent variables (three space variables and a time variable) have to be solved. The introduction of time variable into the analysis leads to great difficulties in obtaining solutions to the complete set of boundary layer equations. The review of papers on the theoretical and computational aspects of the unsteady boundary layers has recently been given by Cousteix [1] and Bettess et al. [2]. Also the boundary layer equations may blow up after certain time [3] due to the increase in the boundary layer thickness with time. Therefore, many investigators have considered similar solutions while studying the three-dimensional boundary layer phenomena. The steady laminar compressible three-dimensional boundary layers at the stagnation point was considered by Libby [4] and the corresponding unsteady case was investigated by Kumari and Nath [5]. Reshotko and Beckwith [6] studied the steady compressible boundary layer flow over an infinite swept cylinder, whereas Sau and Nath [7] examined the corresponding unsteady phenomenon. Dwyer [8] discussed in detail certain aspects of the three-dimensional boundary layers. Peake et al. [9] studied the three-dimensional flow separation on aircrafts and missiles, whereas Smith [10] analysed the phenomena of flow separation associated with the three-dimensional boundary layers.

The boundary layer flow on a cone at an angle of attack near a plane of symmetry is a three-dimensional flow which has several interesting features. There can be a pressure gradient, either favourable or adverse, in the plane of symmetry and either inflow into or outflow from that plane. The study of boundary layer flow on a body of revolution at an angle of incidence near the windward and leeward generators is important in the design of missiles and re-entry vehicles. The boundary layer flow on a cone at an angle of attack near the windward plane of symmetry was studied by Moore [11, 12] and Reshotko [13], whereas Trella and Libby [14], Murdock [15], Roux [16], Wu and Libby [17] and Rubin et al. [18] considered both the windward and leeward sides. These studies showed the existence of non-unique solutions for both outflow and inflow. Chou [19] described an approximate method for the solution of three-dimensional boundary layers on a cone near the plane of symmetry. Lin and Rubin [20] have presented a detailed study of three-dimensional compressible boundary layer flow over a cone at an angle of attack. Nomura [21] has obtained similarity solutions of the boundary layer flow over the leeward side of a yawed blunted cone. Wortman [22] carried out a parameteric study of laminar boundary layer flows with variable fluid properties, non-unity Prandtl number viscous dissipation and obtained similarity solutions at the windward generators of sharp cones at angles of attack.

All the above studies dealt with the steady flows where self-similar solutions were obtained. For simplicity they (except [22]) have taken the product of density and viscosity to be constant ($\rho\mu =$ constant) and the Prandtl number $\mathrm{Pr} = 1$. As mentioned earlier, the flow is likely to be unsteady as in the case of entry or re-entry space vehicles which undergo deceleration, supersonic aircrafts where the speed is suddenly changed, and rockets and missiles where the angle of attack is impulsively changed. In recent years, the unsteady laminar compressible boundary layers over two-dimensional and axi-symmetric bodies have been studied by a few investigators [23–25].

The performance criteria associated with satellites, space vehicles, aircrafts etc. strongly depend on the thickening boundary layer and the subsequent shock wave separation which explicitly influences the point of transition in the viscous layer from laminar to turbulent

resulting in an increase in the drag. One of the tools for controlling this undesirable feature is to apply suction on the surface. Even a small amount of suction reduces the boundary layer thickness in the separation region.

This analysis aims to study the unsteady laminar viscous hypersonic flow over a permeable cone at an angle of attack near the plane of symmetry. The flow is assumed to be steady at time $t=0$ and at time $t>0$ it becomes unsteady due to the free stream velocity which varies arbitrarily with time. We have included the effect of suction to retard the growth of the boundary layers. We have considered variable fluid properties, non-unity Prandtl number and viscous dissipation. The nonlinear coupled parabolic partial differential equations governing the unsteady boundary layer flow over a cone have been solved by using an implicit finite-difference method. The steady-state results without suction have been compared with those of Wu and Libby [17] and Wortman [22]. The present work is an extension of the work of Wu and Libby [17] to include the effects of unsteadiness, suction, viscous dissipation, variable fluid properties and non-unity Prandtl number and of Wortman [22] to include the effect of unsteadiness. The results will be useful in reducing the drag on aircrafts, satellites, missiles and space vehicles.

2 Problem formulation

Let us consider the unsteady laminar compressible boundary layer governing the hypersonic flow over a circular cone at an angle of incidence near a plane of symmetry. The flow is steady initially (i.e., at time $t=0$) and it becomes unsteady at $t>0$ due to the change in the free stream velocity which varies arbitrarily with time. This introduces unsteadiness in the flow field. Figure 1 shows the coordinate system (x, z, $r\theta$), where x is the distance along a generator of the cone from apex, z the distance normal to the surface, $r=r(x)$ the cylindrical radius of the cone and θ is the circumferential angle. The corresponding velocity components are u, w and v. We have assumed variable fluid and non-unity Prandtl number ($\rho \propto T^{-1}$, $\mu \propto T^{\omega}$, $\mathrm{Pr} \neq 1$, where ρ, μ and T are density, viscosity and temperature of the fluid, respectively, and ω is the index in the power-law variation of the viscosity), and included viscous dissipation terms in the energy equation. We have also taken the Prandtl number, Pr, to be constant across the boundary layer, because in most of the atmospheric flight problems its variation is small [26]. We consider the plane of symmetry to be $\theta=0$ and assume expansions in θ for the velocity components u, v and w, the total enthalpy, H, and the static pressure p appropriate to the plane of symmetry (i.e., u, w, H and p are even functions and v odd function). Using these expansions into the unsteady boundary layer equations for conservation of mass, of x-wise and θ-wise momentum, and of energy and considering only zero-order and first-order terms in θ, we obtain the following system of equations [17, 27, 28]

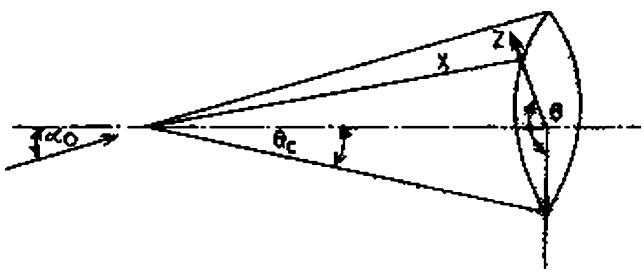

Fig. 1 Physical model and coordinate system

$$\frac{\partial(\rho r)}{\partial t}+\frac{\partial(\rho u r)}{\partial x}+\rho v+r\frac{\partial(\rho w)}{\partial z} = 0, \tag{1}$$

$$\rho\left(\frac{\partial u}{\partial t}+u\frac{\partial u}{\partial x}+w\frac{\partial u}{\partial z}\right)=-\frac{\partial p_0}{\partial x}+\frac{\partial}{\partial z}\left(\mu\frac{\partial u}{\partial z}\right), \tag{2}$$

$$\rho\left(\frac{\partial v}{\partial t}+u\frac{\partial v}{\partial x}+\frac{v^2}{r}+w\frac{\partial v}{\partial z}\right)=-\frac{2p_0}{r}+\frac{\partial}{\partial z}\left(\mu\frac{\partial v}{\partial z}\right), \tag{3}$$

$$\rho\left(\frac{\partial H}{\partial t}+u\frac{\partial H}{\partial x}+w\frac{\partial H}{\partial z}\right) = \frac{\partial p_0}{\partial t}+\frac{\partial}{\partial z}\left[\frac{\mu}{\mathrm{Pr}}\frac{\partial H}{\partial z}+\left(1-\overset{-1}{\mathrm{Pr}}\right)\mu u\frac{\partial u}{\partial z}\right], \tag{4}$$

where

$$\begin{aligned} &-\tfrac{\partial p_0}{\partial x}=\rho_e\tfrac{\partial u_e}{\partial t}+\rho_e\, u_e\tfrac{\partial u_e}{\partial x},\\ &-2p_2=\rho_e x\sin\theta_c\tfrac{\partial v_e}{\partial t},\quad r=x\sin\theta_c,\\ &\qquad +\rho_e u_e\sin\theta_c x\tfrac{\partial v_e}{\partial x}+\rho_e v_e^2,\\ &\tfrac{\partial p_0}{\partial t}=\rho_e\left(\tfrac{\partial H_e}{\partial t}+\ u_e\tfrac{\partial H_e}{\partial x}\right),\ H=h+u^2/2. \end{aligned} \tag{5}$$

The boundary conditions are

$$\begin{aligned} &u=v=0,\quad w=w\gamma_w,\quad H=H_w \text{ at } z=0,\quad t>0,\\ &u=u_e=u_0R(t^*),\quad v=v_e=v_0R(t^*),\quad H=H_e \text{ as } z\to\infty. \end{aligned} \tag{6}$$

The initial conditions are given by

$$u=u_i,\quad v=v_i,\quad w=w_i,\quad H=H_i \text{ at } t=0. \tag{7}$$

Here r is the cylindrical radius of the cone, t the time, $\tau(=(3/2)\,(u_0/x)t)$ the dimensionless time, ρ the density of the fluid, μ the fluid viscosity, Pr is the Prandtl number, v now denotes the velocity gradient in the direction normal to the plane of symmetry and the actual velocity either into ($v<0$) or out of ($v>0$) the plane of symmetry is $v\theta$, whereas the cross flow velocity is given by v/v_e [17], p is the static pressure, p_0 is the static pressure at the plane of symmetry ($\theta=0$), p_2 denotes the curvature of the pressure distribution along the plane of symmetry, u_e and v_e are the velocity components at the edge of the boundary layer along the x-direction and the θ-direction, respectively and u_0 and v_0 are their values at time t = 0, w_w is the fluid velocity normal to the surface, θ_c is the semi-vertical angle of the cone, h the specific enthalpy, H

the total enthalpy, $R(\tau)$ is a continuous function of dimensionless time τ having continuous first-order derivative with respect to time τ and the subscripts e, i and w denote conditions at the edge of the boundary layer, initial conditions and conditions at the wall, respectively.

Since the flow at the edge of the boundary layer is assumed to be homentropic, the total enthalpy H_e is constant in the inviscid region at the edge of the boundary layer. Hence $\partial p_0/\partial t = 0$.

In order to reduce the number of independent variables from three to two and number of equations from four to three, we apply the following transformations to Eqs. 1, 2, 3, 4

$$\begin{aligned}
&\eta = \left(\frac{3}{2}\frac{\rho_e u_0}{\mu_e x}\right)^{1/2} \int_0^z \frac{\rho}{\rho_e}\mathrm{d}z, \ \xi = 3^{-1}\rho_e\mu_e u_0(\sin\theta_c)^2 x^3,\\
&\tau = (3/2)(u_0/x)t, \quad u(x,z,t) = u_0 R(\tau) f'(\eta,\tau),\\
&v(x,z,t) = v_0 R(\tau) s'(\eta,\tau), H(x,z,t) = H_e g(\eta,\tau),\\
&\alpha = 2\xi v_0/(\rho_e\mu_e u_0^2 r^3) = (2v_0/3u_0 \sin\theta_c),\\
&\beta = (2\xi/v_0 x)\,\mathrm{d}(v_0 x)/\mathrm{d}\xi, \quad f(0,\tau) = A/R(\tau), \quad A = -\left(\frac{3}{2}\right)^{1/2}\frac{(\rho w)_w}{\rho_e u_0}\mathrm{Re}_x^{1/2},\\
&Ec = u_0^2/2He = 2^{-1}(\gamma-1)M_e^2/\left[1+2^{-1}(\gamma-1)M_e^2\right], \quad \mathrm{Re}_x = u_0 x/v_e,\\
&\rho_e/\rho = h/h_e = \left(g - Ec f'^2\right)/(1-Ec), \quad \mu/\mu_e = (h/h_e)^\omega = \left[\left(g - Ec f'^2\right)/(1-Ec)\right]^\omega,\\
&N = \rho\mu/\rho_e\mu_e = \left[\left(g - Ec f'^2\right)/(1-Ec)\right]^{\omega-1}.
\end{aligned} \tag{8}$$

From eq. 8, the cross flow parameter α is a constant if v_0/u_0 is a constant and the parameter $\beta = 2/3$.

Using the transformations given in (8), we first obtain ρw from (1) and use it in (2) – (4). This results in the following equations:

$$(Nf'')' + R(\tau)(f+\alpha s)f'' + R^{-1}(\mathrm{d}R/\mathrm{d}\tau) \times (\rho_e/\rho - f') - \partial f'/\partial\tau = 0, \tag{9}$$

$$\begin{aligned}
&(Ns'')' + R(\tau)(f+\alpha s)s'' + \alpha R(\tau)\left(\rho_e/\rho - s'^2\right)\\
&\quad + (2/3)R(\tau)(\rho_e/\rho - f's')\\
&\quad + R^{-1}\mathrm{d}R/\mathrm{d}\tau(\rho_e/\rho - s') - \partial s'/\partial\tau = 0,
\end{aligned} \tag{10}$$

$$\begin{aligned}
&\left(\overset{-1}{\mathrm{Pr}}Ng'\right)' + R(\tau)(f+\alpha s)g'\\
&\quad + Ec R^2(\tau)\left[\left(1-\overset{-1}{\mathrm{Pr}}\right)Nf'f''\right]' - \partial g/\partial\tau\\
&\quad = 0,
\end{aligned} \tag{11}$$

with boundary conditions

$$\begin{aligned}
&f(0,\tau) = A/R(\tau), \quad f'(0,\tau) = s(0,\tau) = s'(0,\tau) = 0,\\
&g(0,\tau) = g_w, f'(\infty,\tau) = s'(\infty,\tau) = g(\infty,\tau) = 1.
\end{aligned} \tag{12}$$

The initial conditions are given by the steady-state equations which can be obtained from Eqs. 9, 10, 11 by putting $\tau = \mathrm{d}R/\mathrm{d}\tau = \partial f'/\partial\tau = \partial s'/\partial\tau \ \partial g/\partial\tau = 0$ and $R(\tau) = 1$. Consequently, we get the following system of ordinary differential equations governing the steady flow

$$(Nf'')' + (f+\alpha s)f'' = 0, \tag{13}$$

$$\begin{aligned}
&(Ns'')' + (f+\alpha s)s'' + \alpha\left(\rho_e/\rho - s'^2\right)\\
&\quad + (2/3)(\rho_e/\rho - f's') = 0,
\end{aligned} \tag{14}$$

$$\left(\mathrm{Pr}^{-1}Ng'\right)' + (f+\alpha s)g' + Ec\left[\left(1-\mathrm{Pr}^{-1}\right)Nf'f''\right]' = 0 \tag{15}$$

with boundary conditions

$$\begin{aligned}
&f(0) = A, \ f'(0) = s(0) = s'(0) = 0, \ g(0) = g_w,\\
&f'(\infty) = s'(\infty) = g(\infty) = 1.
\end{aligned} \tag{16}$$

Here η and ξ are transformed coordinates, τ the dimensionless time, f' the dimensionless velocity in the streamwise direction, s′ is the dimensionless velocity gradient in the direction normal to the plane of symmetry, g the dimensionless total enthalpy, g_w the total enthalpy at the wall, Re_x the Reynolds number, α the cross flow parameter, β the parameter associated with the three-dimensional nature of the flow, Ec the viscous dissipation parameter, N is the product of the density–viscosity ratios, ω the index in the power-law variation of the viscosity and $\omega = 0.5$ for the hypersonic flow, $\omega = 0.7$ for the supersonic flow and $\omega = 1$ when the density–viscosity product $\rho\mu$ is a constant (this simplification has been widely used in the literature), M_e is the Mach number at the edge of the boundary layer and prime denotes derivative with respect to η. If the fluid velocity normal to the surface is a constant (i.e., $(\rho w)_w/\rho_e u_0$ is a constant), then the mass transfer parameter A is a constant for a fixed Reynolds number and $A > 0$ for suction (here we have considered only suction).

It may be remarked the steady-state Eqs. 13, 14, 15 under conditions (16) for $A=0$ (no suction), $\mathrm{Pr}=N=\omega=1$, $\mathrm{Ec}=0$ are identical to those of Wu and Libby [17] and for $A \neq 0$, $N \neq 1$, $\omega \neq 1$ to those of Wortman [22].

3 Methods of solution

Equations 9, 10, 11 under boundary conditions (Eq. 12) and initial conditions (Eqs. 13, 14, 15, 16) have been solved by using an implicit, tridiagonal iterative finite-difference scheme similar to that of Blottner [29]. All the first-order derivatives with respect to τ are replaced by two-point backward-difference formulae

$$\partial L/\partial\tau = \left(L_{m,n} - L_{m-1,n}\right)/\Delta\tau, \tag{17}$$

where L denotes any dependent variable f' or s' or g and m and n are node locations along τ and η directions, respectively. First the third-order partial differential Eqs 9, and 10 are converted to second-order by substituting $f'=F$ and $s'=S$. Then these second-order partial differential equations are descretised by three-point central difference formulae and all the first order by trapezoidal rule. The terms f and s are evaluated from $f=f(0,\tau)+\int_0^n F\mathrm{d}\eta$ and $s=s(0,\tau)+\int_0^n S\mathrm{d}\eta$. The nonlinear terms are evaluated at the previous iteration. At each time step of constant τ, a system of algebraic equations are solved iteratively by using the Thomas algorithm (see, Blottner [29]). The same procedure is repeated for the next τ value and the equations are solved line by line until the desired value of τ is reached. A convergence criterion based on the relative difference between the current and previous iterations is used. When this difference reaches 10^{-5}, the solution is assumed to have converged and the iterative process is terminated.

A sensitivity analysis of the effect of the step sizes $\Delta\eta$ and $\Delta\tau$ and the edge of the boundary layer η_∞ on the solutions was performed. Finally, the computations were carried out with $\Delta\eta=0.02$, $\Delta\tau=0.005$ for $0 \leq \tau \leq 0.2$ and $\Delta\tau=0.05$ for $0.2<\tau \leq 2.0$ and $\eta_\infty=8$.

4 Results and discussion

Equations 9, 10, 11 under boundary conditions (Eq. 12) and initial conditions (Eqs. 13, 14, 15, 16) have been solved by using an implicit finite-difference scheme as described earlier. In order to validate our results, we have compared the steady state surface shear stresses in the streamwise and cross flow directions ($f''(0)$, $s''(0)$) for $A=\mathrm{Ec}=0$, $\mathrm{Pr}=N=\omega=1$ with those of Wu and Libby [17] and they are found to be in good agreement. The comparison is shown in Figs. 2 and 3. We have also compared the ratio of surface shear stresses in the streamwise and cross flow directions and the surface heat transfer for the steady state ($f''(0)/f_0''(0)$,$s''(0)/s_0''(0)$,$g'(0)/g'_0(0)$, where $f''(0)$, $s''(0)$ and $g'(0)$ are surface shear stresses and heat transfer on a cone for an angle of attack and $f''_0(0)$, $s''_0(0)$ and $g'_0(0)$ are corresponding results for zero angle of attack) when $\omega=0.5$, $\mathrm{Ec}=0.5$, $g_\mathrm{w}=0.1$, $0 \leq \alpha \leq 3$, $\mathrm{Pr}=0.715$ with those of Wortman [22] and found them in very good agreement. The comparison is presented in Table 1.

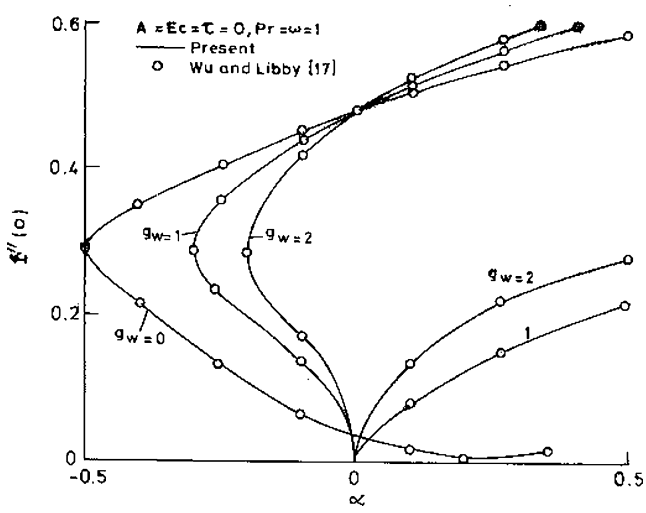

Fig. 2 Comparison of streamwise surface shear stress for the steady flow, $f''(0)$, when $A=0$, $\mathrm{Pr}=\omega=1$, $\mathrm{Ec}=0$ with that of Wu and Libby [17]

The effects of the cross-flow parameter α on the velocity and total enthalpy profiles($f'(\eta,\tau)$, $s'(\eta,\tau)$, $g(\eta,\tau)$) for $A=2$, $g_\mathrm{w}=0.25$ $M_\mathrm{e}=20$, $\mathrm{Pr}=0.7$, $R(\tau)=1+\varepsilon\tau^2$, $\varepsilon=0.2$, $\gamma=1.4$, $\omega=0.5$, $\tau=1.0$ are shown in Figs. 4, 5, 6. The velocity and the total enthalpy profiles increase with α. However, the effect is more pronounced on the cross-flow velocity profiles ($s'(\eta,\tau)$) than on the streamwise velocity profiles $f'(\eta,\tau)$ and the total enthalpy profiles $g(\eta,\tau)$, because α produces more significant changes on

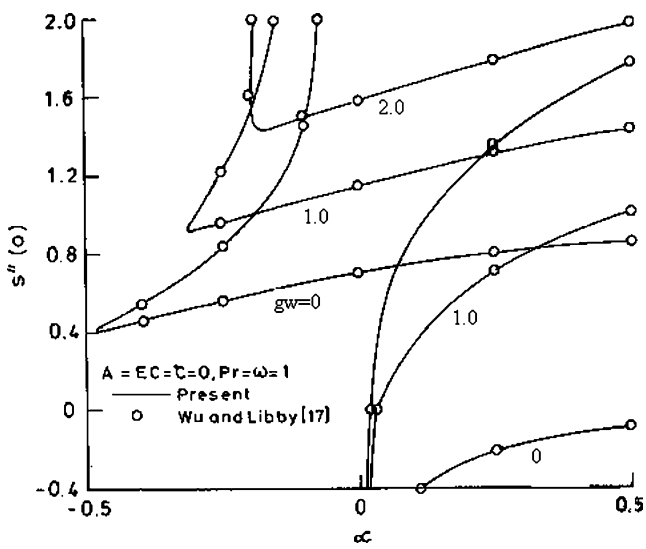

Fig. 3 Comparison of cross flow surface shear stress for the steady flow, $s''(0)$, when $A=0$, $\mathrm{Pr}=\omega=1$, $\mathrm{Ec}=0$ with that of Wu and Libby [17]

Table 1 Comparison of the ratio of surface shear stresses and heat transfer for $g_w = 0.1$, Ec = 0.5, Pr = 0.715, $w = 0.5$, $A = 0$

α	Present results			Wortman [22]		
	$f''(0)/f''_0(0)$	$s''(0)/s''_0(0)$	$g'(0)/g'_0(0)$	$f'(0)/f''_0(0)$	$s''(0)/s''_0(0)$	$g'(0)/g'_0(0)$
0	1.00	1.00	1.00	1.00	1.00	1.00
0.5	1.302	1.281	1.301	1.30	1.28	1.30
1.0	1.541	1.510	1.530	1.54	1.51	1.53
2.0	1.921	1.892	1.921	1.92	1.89	1.92
3.0	2.249	2.199	2.242	2.25	2.20	2.24

$s'(\eta,\tau)$ than on $f'(\eta,\tau)$ and $g(\eta,\tau)$. Also, there is an overshoot in the cross-flow velocity profiles ($s'(\eta,\tau)$) near the surface if $\alpha > \alpha_0$. Further increase in α enhances the magnitude of velocity overshoot.

The effects of the cross-flow parameter α on the streamwise surface shear stress ($f''(o,\tau)$) and the cross-flow surface shear stress ($s''(o,\tau)$) and the surface heat transfer ($g'(o,\tau)$) are presented in Figs. 7, 8, 9. Since positive α acts like a favourable pressure gradient and negative α as an adverse pressure gradient, for a fixed time τ, the surface shear stresses and the heat transfer increase with α, but the effect is more pronounced on the cross-flow shear stress. For $\tau = 1$, the cross-flow shear stress for $\alpha = 1.0$ is about seven times its value for $\alpha = -1.0$. For a fixed α, the surface shear stress in the streamwise direction ($f''(0, \tau)$) increases monotonically with time τ. For $\alpha = 1$, $f''(0,\tau)$ increases by about 55% as α increases from -1 to 1. On the other hand, the cross-flow surface shear stress and the surface heat transfer ($s''(0,\tau)$, $g'(0,\tau)$) do not change with time monotonically. The cross flow surface shear stress for $\tau \geq 0$ decreases in the time interval $0 \leq \tau \leq 0.5$ and then slowly increases, but for $\alpha > 0$, it increases with time τ in general. The surface heat transfer ($g'(0, \tau)$) first increases in the interval $0 \leq \tau \leq 0.5$ and then decreases. The trend mentioned above is due to the opposite role played by the parameters.

Figures 10, 11, 12 present the effects of surface suction ($A > 0$) on the velocity and total enthalpy profile ($f'(\eta,\tau)$, $s'(\eta,\tau)$, $g(\eta,\tau)$) for $g_w = 0.25$, $M_e = 20$, Pr = 0.7, $\alpha = 0.5$, $R(\tau) = 1 + \varepsilon\tau^2$, $\varepsilon = 0.2$, $\gamma = 1.4$, $\omega = 0.5$, $\tau = 1.0$.

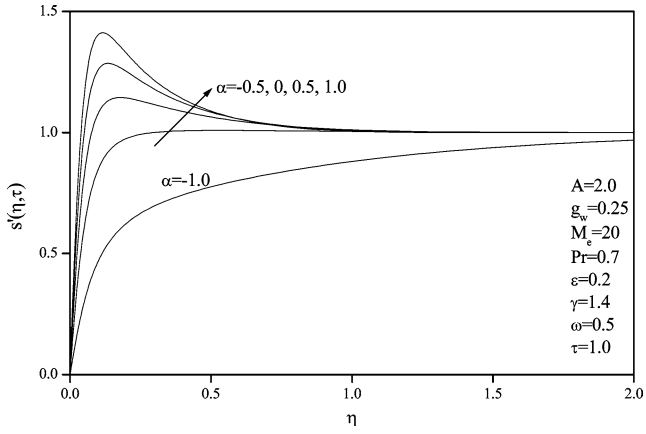

Fig. 5 Effects of cross flow parameter α on $s'(\eta,\tau)$

Since suction reduces the momentum and thermal boundary thicknesses, the velocity and total enthalpy profiles increase with A. Suction also increases the overshoot in the cross flow velocity.

Figures 13, 14, 15 display the effects of suction ($A > 0$) on the streamwise and cross-flow surface shear stresses ($f''(0,\tau)$, $s''(0,\tau)$) and the surface heat transfer ($g'(0,\tau)$) for $g_w = 0.25$, $M_e = 20$, Pr = 0.7, $\alpha = 0.5$, $R(\tau) = 1 + \varepsilon\tau^2$, $\varepsilon = 0.2$, $\gamma = 1.4$, $\omega = 0.5$, $0 \leq \tau \leq 2.0$. Since suction suck away the hot fluid near the surface, it provides a stabilising effect on the flow field and reduces the momentum and thermal boundary layers. Consequently, for a given time τ, the streamwise and cross-flow shear

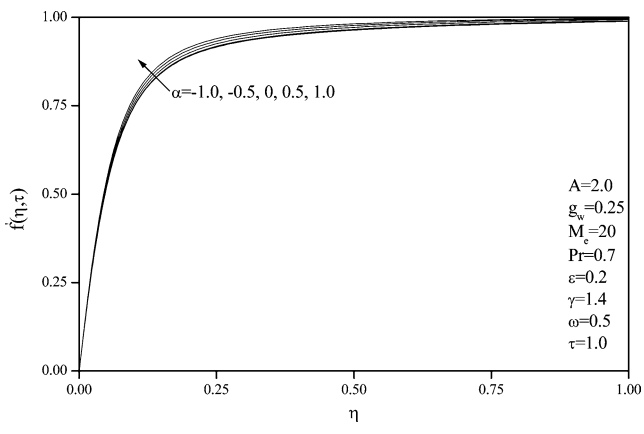

Fig. 4 Effects of cross flow parameter α on $f'(\eta,\tau)$

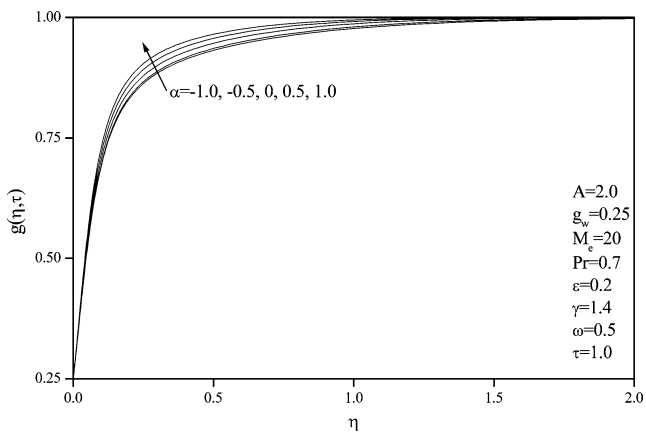

Fig. 6 Effects of cross flow parameter α on $g(\eta,\tau)$

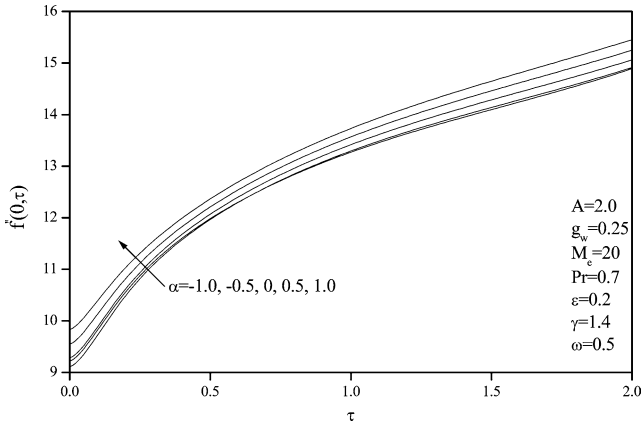

Fig. 7 Effects of cross flow parameter α on $f''(0, \tau)$

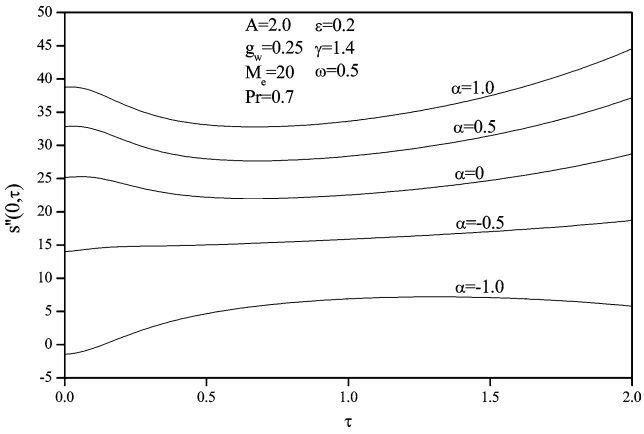

Fig. 8 Effects of cross flow parameter α on $s''(0, \tau)$

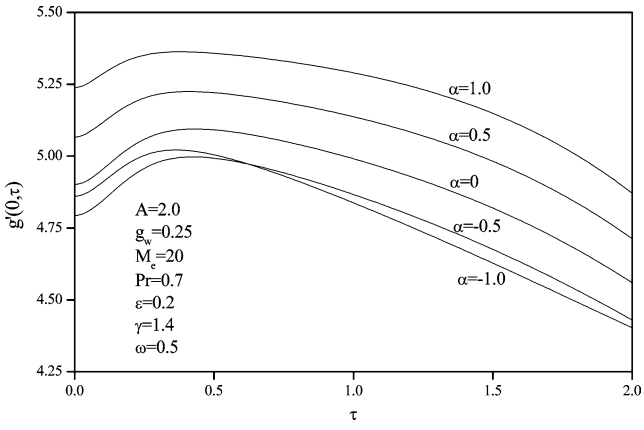

Fig. 9 Effects of cross flow parameter α on $g'(0,\tau)$

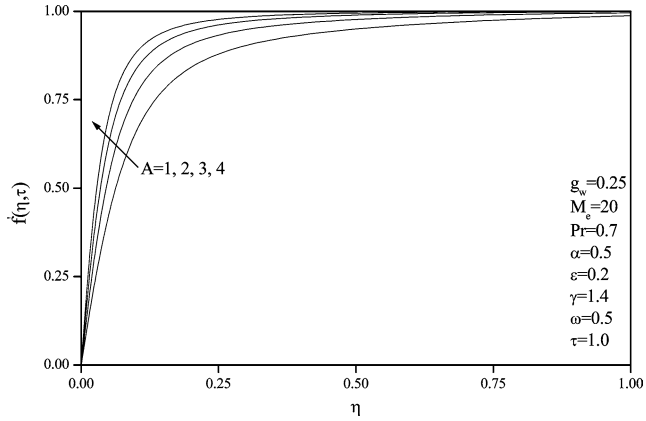

Fig. 10 Effects of suction parameter A on $f'(\eta,\tau)$

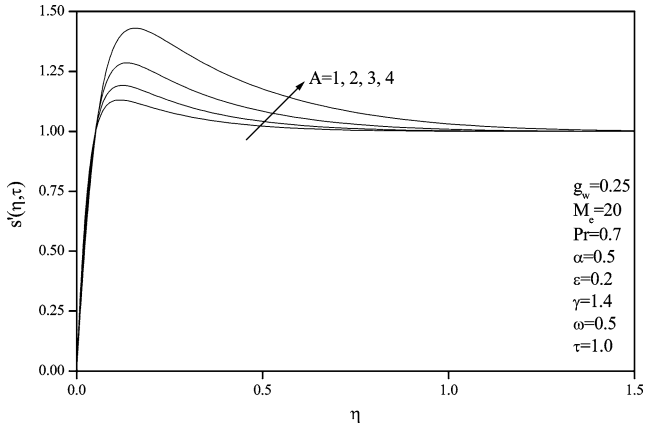

Fig. 11 Effects of suction parameter A on $s'(\eta,\tau)$

stresses and the heat transfer increase with A. However, in a small interval of time ($0 \leq \tau \leq 0.2$) the cross-flow shear stress differs from this trend due to the competition amongst various parameters having opposing trends. At time $\tau = 2$, the streamwise surface shear stress, cross-flow surface shear stress and heat transfer increase by 110, 40 and 276%, respectively. For a given A, the surface shear stress in the streamwise direction ($f''(0,\tau)$) increase monotonically with time τ. When $A = 2$, $f''(0,\tau)$ increases by about 58% as τ increases from zero to two. On the other hand, the variation of the cross-flow surface shear stress ($s''(0,\tau)$) and the surface heat transfer

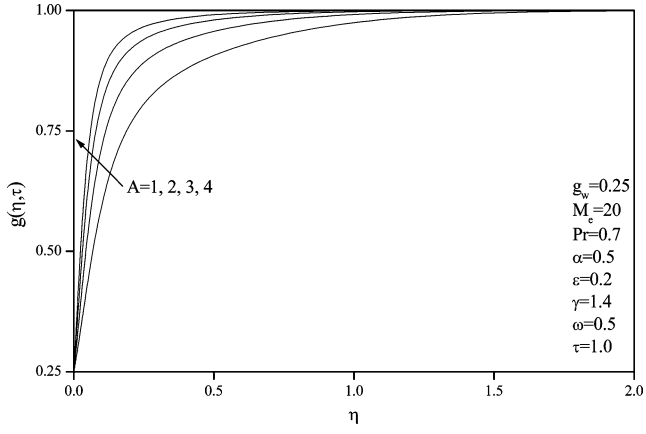

Fig. 12 Effects of suction parameter A on $g(\eta,\tau)$

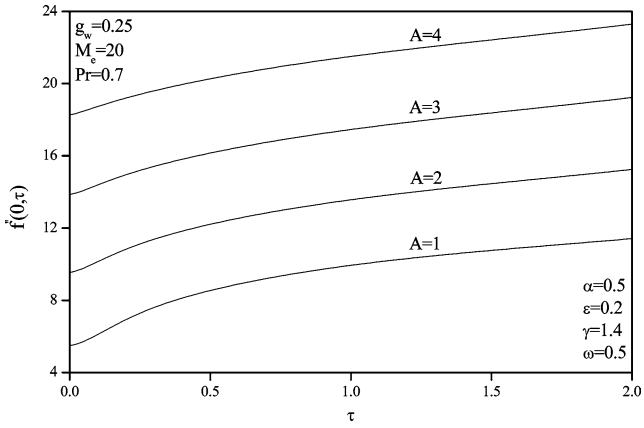

Fig. 13 Effects of suction parameter A on $f''(0,\tau)$

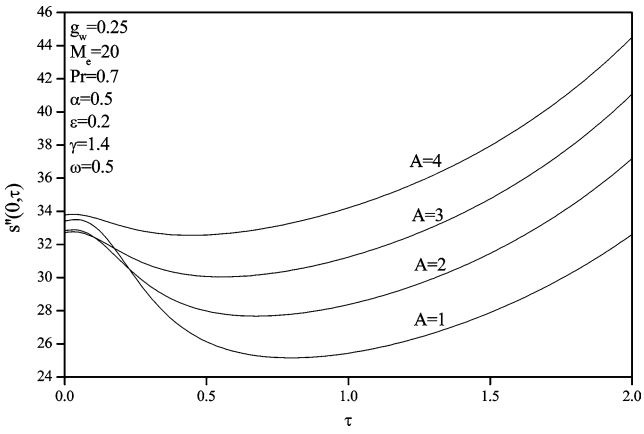

Fig. 14 Effects of suction parameter A on $s''(0,\tau)$

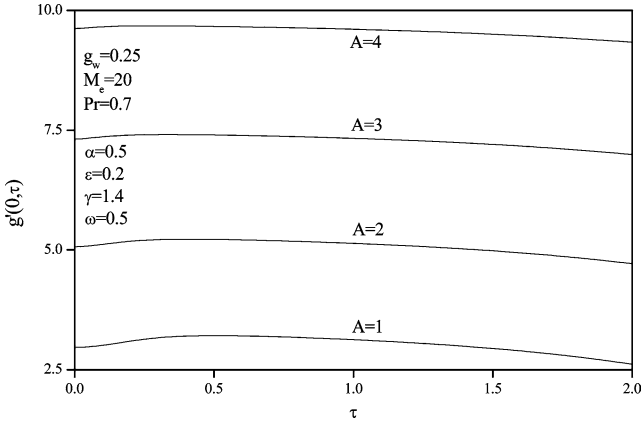

Fig. 15 Effects of suction parameter A on $g'(0, \tau)$

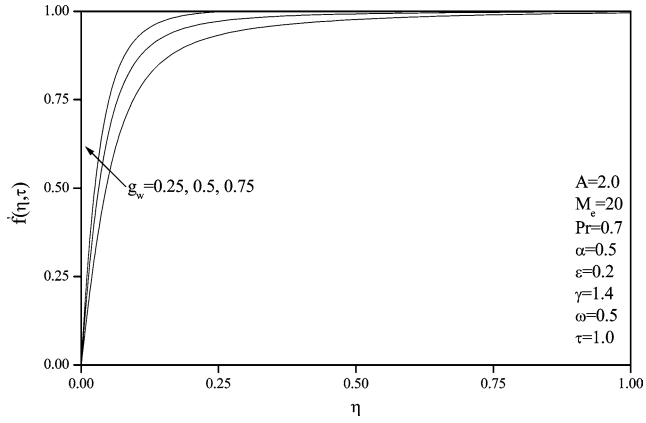

Fig. 16 Effects of total enthalpy at the wall g_w on $f'(\eta,\tau)$

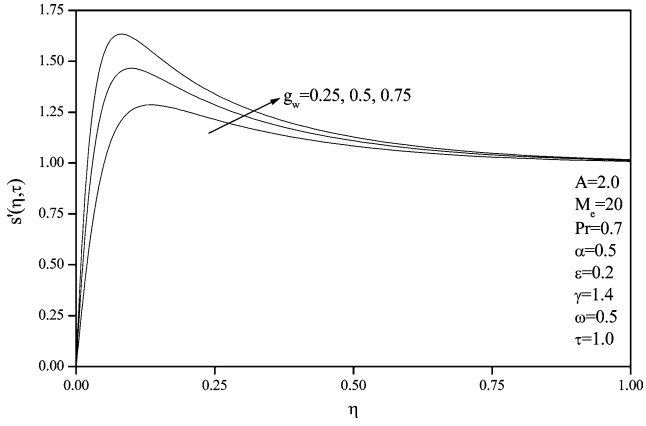

Fig. 17 Effects of total enthalpy at the wall g_w on $s'(\eta,\tau)$

($g'(0,\tau)$) with time τ is non-monotonic. The cross-flow surface shear stress first decreases with increasing time τ and attains a minimum in the time interval $0.4 < \tau < 0.75$ depending on the value of A. The location of this minimum shifts towards the wall as A increases. The surface heat transfer qualitatively shows trend opposite to that of cross-flow shear stress. Also it varies very little with time.

The effects of the total enthalpy g_w at the wall on the velocity and total enthalpy profiles ($f'(\eta,\tau)$, $s'(\eta,\tau)$, $g(\eta,\tau)$) for $A = 2$, $M_e = 20$, $\Pr = 0.7$, $\alpha = 0.5$, $R(\tau) = 1 + \varepsilon\tau^2$, $\varepsilon = 0.2$, $\tau = 1.0$, $\gamma = 1.4$, $\omega = 0.5$ are shown in Figs. 16, 17,

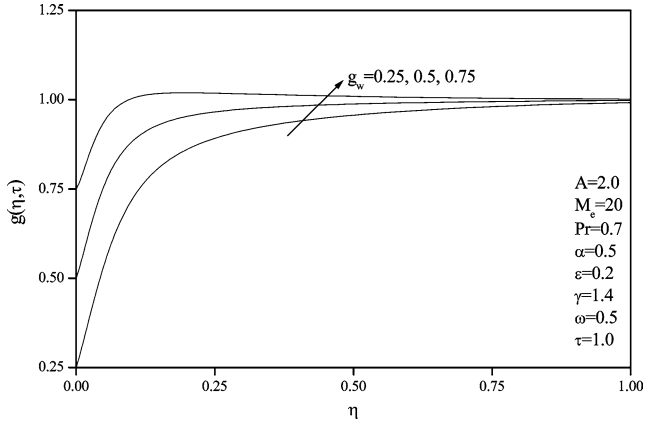

Fig. 18 Effects of total enthalpy at the wall g_w on $g(\eta,\tau)$

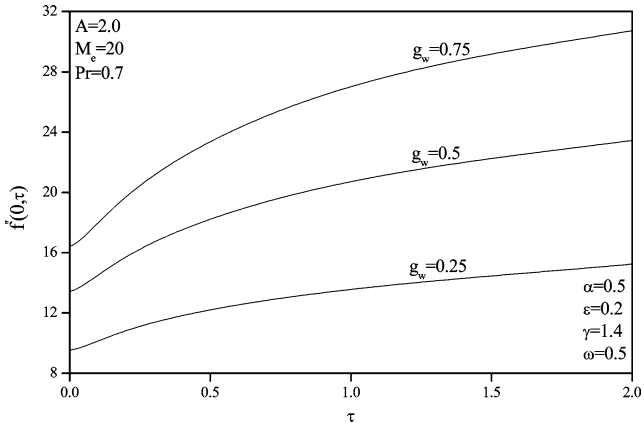

Fig. 19 Effects of total enthalpy at the wall g_w on $g''(0, \tau)$

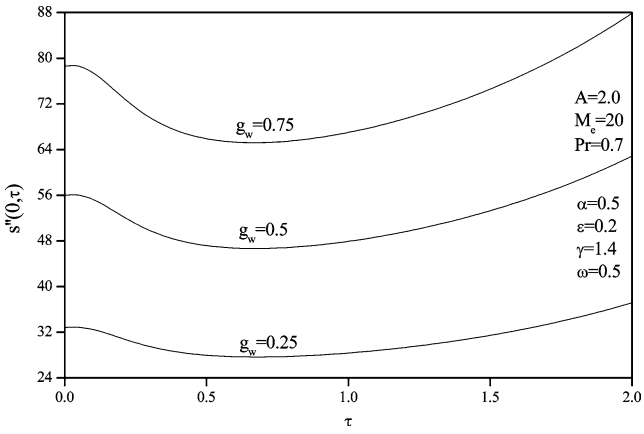

Fig. 20 Effects of total enthalpy at the wall g_w on $s''(0, \tau)$

18. It is evident from these figures that both the velocity and the total enthalpy profiles increase with g_w everywhere. Consequently, velocity gradients in the streamwise and cross-flow directions increase with g_w, but the total enthalpy gradient decreases. This can be explained as follows. When g_w increases, the wall becomes more hot, but the total enthalpy difference between the fluid near and at the wall decreases. This in turn causes reduction in the total enthalpy gradient at the surface. For $g_w = 0.75$, the total enthalpy ($g(\eta,\tau)$) near the wall slightly exceeds its value at the edge of the boundary layer (overshoot in the total enthalpy profiles). This overshoot is attributed to the simultaneous effects of various parameters.

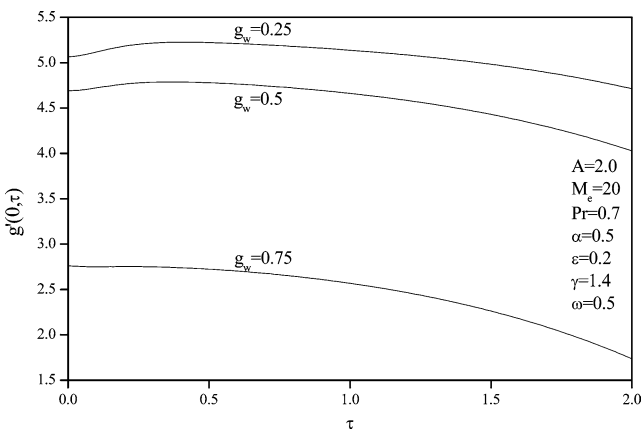

Fig. 21 Effects of total enthalpy at the wall g_w on $g'(0, \tau)$

Figures 19, 20, 21 show the effects of the total enthalpy at the wall g_w on the surface shear stresses in the streamwise and cross-flow directions ($f''(0,\tau)$, $s''(0,\tau)$) and the surface heat transfer ($g'(0,\tau)$) for $A = 2$, $M_e = 20$, $\Pr = 0.7$, $\omega = 0.5$, $R(\tau) = 1 + \varepsilon\tau^2$, $\varepsilon = 0.2$, $0 \leq \tau \leq 2$, $\gamma = 1.4$, $\alpha = 0.5$. As in the case of suction parameter A, the surface shear stresses in the streamwise and cross-flow directions ($f''(0,\tau)$, $s''(0,\tau)$) for a fixed time τ increase with g_w, but unlike suction the surface heat transfer ($g'(0,\tau)$) decreases. This last trend is due to the reduction of the total enthalpy gradient with increasing g_w. For $\tau = 2$, $f''(0,\tau)$, $s''(0,\tau)$ and $g'(0,\tau)$ increase by about 105, 160 and 174% as g_w increases from 0.25 to 0.75. For a fixed g_w, the variation of the surface shear stresses and the heat transfer ($f''(0,\tau)$, $s''(0,\tau)$, $g'(0,\tau)$) with time τ is qualitatively similar to that of the suction parameter A. Hence it is not discussed here.

5 Conclusions

The total enthalpy at the wall and suction strongly affect the surface shear stresses in the streamwise and cross-flow directions as well as the surface heat transfer and they increase with these parameters except the heat transfer which decreases with increasing wall enthalpy. The cross-flow parameter significantly affects the cross-flow surface shear stress, but its effect on the streamwise shear stress and the heat transfer is comparatively weak. There is an overshoot in the cross-flow velocity when the cross flow parameter exceeds a certain value and the magnitude of this overshoot increases with cross-flow parameter, suction and total enthalpy at the wall. When the total enthalpy at the wall exceeds a certain value, slight overshoot in the total enthalpy profile occurs. The role of suction is found to be very important in the sense that it enables us to obtain unique solution.

References

1. Cousteix J (1986) Three dimensional and unsteady boundary layer computations, Ann Rev Fluid Mech 18:173–200
2. Bettess R, Watts J, Balkema AA (1992) Unsteady flow and fluid transients. Netherlands Publishers
3. Childress S, Ierly R, Spiegel EA, Young WR (1989) Blow up of unsteady two-dimensional Euler and Navier–Stokes solutions having stagnation point form. J Fluid Mech 203:1–22
4. Libby PA (1967) Heat and mass transfer at a general three-dimensional stagnation point. AIAA J 5:507–517

5. Kumari M, Nath G (1978) Unsteady laminar compressible boundary layer flow at a three-dimensional stagnation point. J Fluid Mech 87: 708–718
6. Reshotko E, Beckwith IE (1958) Compressible laminar boundary layer over a yawed infinite cylinder with heat transfer and arbitrary Prandtl number, TN1379, NACA
7. Sau A, Nath G (1995) Unsteady compressible boundary layer flow on the stagnation line of an infinite swept cylinder, Acta Mech 108:143–156
8. Dwyer HA (1981) Some aspects of three-dimensional laminar boundary layers. Ann Rev Fluid Mech 13:217–229
9. Peake DJ (1972) Three dimensional flow separation on aircrafts and missiles. AIAA J 10:567–575
10. Smith FJ (1980) A three-dimensional boundary layer separation. J Fluid Mech 99:185–195
11. Moore FK (1951) Laminar boundary layer on circular cone in supersonic flow at small angle of attack, TN 2521, NACA
12. Moore FK (1952) Laminar boundary layer at large angle of attack, TN 2844, NACA
13. Reshotko E (1957) Laminar boundary layer with heat transfer on a cone at angle of attack in a supersonic stream, TN 4152, NACA
14. Trella M, Libby PA (1965) Similar solutions for the hypersonic laminar boundary layer near a plane of symmetry. AIAA J 3:75–83
15. Murdock JW (1972) The solution of sharp cone boundary layer equations in the plane of symmetry. J Fluid Mech 54:665–678
16. Roux B (1972) Supersonic laminar boundary layer near the plane of symmetry of a cone at incidence. J Fluid Mech 51:1–14
17. Wu P, Libby PA (1973) Laminar boundary layer on a cone near a plane of symmetry. AIAA J 11:326–333
18. Rubin SG, Lin TC, Tarulli F (1977) Symmetry plane viscous layer on a sharp cone. AIAA J 15:204–211
19. Chou YS (1973) Approximate method of solution for three-dimensional boundary layers. AIAA J 11:1025–1028
20. Lin A, Rubin SG (1982) Three-dimensional supersonic viscous flow over a cone at incidence. AIAA J 20:1500–1507
21. Nomura S (1976) Similar boundary layer analysis for lee-surface heating on yawed blunted cone. AIAA J 14:1509–1510
22. Wortman A (1972) Heat and mass transfer on cones at angles of attack. AIAA J 10:832–834
23. Takhar HS, Yano K, Nakamura s, Nath G (1997), Unsteady compressible boundary layer in the stagnation region of a sphere with a magnetic field. Arch Appl Mech 67:478–486
24. Sau A, Nath G (1997) Unsteady compressible boundary layer flow at the stagnation point of a rotating sphere with an applied magnetic field. Arch Mech 49:111–127
25. Subhashini SV, Nath G (1999) Self-similar solution of unsteady laminar compressible boundary layers in the stagnation region of two-dimensional and axisymmetric bodies. Acta Mech 134:135–145
26. Wortman A, Ziegler H, Soo-Hoo G (1971) Convective heat transfer at general three-dimensional stagnation point, Int J Heat Mass Transfer 14:149–152
27. Moore FK (1956) Three-dimensional boundary layer theory, Advances in Applied Mechanics, vol 4. Academic Press, New York, pp 160–224
28. Libby PA, Fox H, Sanator RJ, Decarlo J (1963) Laminar boundary layer near the plane of symmetry of a hypersonic inlet. AIAA J 1:2732–2740
29. Blottner FG (1970) Finite-difference methods of solution of the boundary layer equations. AIAA J 8:193–205